International Conference on Applied Energy 2019
Aug 12-15, 2019, Västerås, Sweden
Paper ID: 0156

COMPARISON OF THE TRANSMISSION OF THE UNCERTAINTY IN THE THEORETICAL MODEL AND DATA-DRIVEN MODEL: TAKE PV FOR EXAMPLE

Hao Li, Jun Zhao*, Minxia Li, Shengyuan Zhong, Wenjia Li, Fuzhong Wang

Key Laboratory of Efficient Utilization of Low and Medium Grade Energy (Tianjin University), Ministry of Education of China, Tianjin 300350, China

ABSTRACT

With the intermittent and unstable renewable power feeding into the district energy systems (DES), the reliability of the system need to be accurately evaluated is of great significance. In order to predict the probability of system operational state in the design stage, in addition to provide the reasonable distributions of the input parameters, the transmission of the uncertainty in the analytical model need to clarify. In this paper, taking photovoltaic systems for example, the method to quantify the meteorological parameters distributions in the uncertainty analysis was proposed. And then the transmission of the uncertainty in the theoretical model and data-driven model were compared. The Back Propagation Neural network model (BP model) was selected as example. The BP model shows high accuracy than theoretical model, meanwhile, it also shows lower uncertainty. The results indicated that the data-driven model is more suitable for estimating the system output in the design stage. The research will provide guidance for system modeling by using data-driven model.

Keywords: district energy systems, uncertainty transmission, theoretical model, BP model, photovoltaic

NONMENCLATURE

Abbreviations	
BP	Back Propagation Neural network
TH	Theoretical
EVA	Ethylene-Vinyl-Acetate
MPPT	Maximum power point
Symbols	
G	solar radiation intensity [W/m^2]
h	heat transfer coefficient [W/m^2 ƙ]/ Planck constant [-]
I	current [A]
$I_{AM1.5}$	standard solar spectrum [-]
k	conductivity [W/m ƙ]
k_I	current temperature coefficient [%/ ℃]
k_V	voltage temperature coefficient [%/ ℃]
k_B	Boltzmann constant [-]
P_{sun}	solar radiation intensity [W/m^2]
P_{rad}	thermal emission intensity [W/m^2]
RH	relative humidity [%]
S	area [m^2]
T	temperature [K]
v	wind speed [m/s]
V	voltage [V]
Subscripts	
cc	open circuit
g	glass cover
PV	photovoltaic cell
sky	sky
sc	short circuit
ted	tedlar
v	convection

1. INTRODUCTION

With the improvement of the renewable energy share in the district energy systems (DES), the effects of the uncertainties in design, arising from a variety of sources such as the random meteorological condition, the incomplete knowledge of the energy demand, the approximate parametric hypothesis and mathematical model, limit the accuracy of the simulation results. The uncertainty modeling and research in the DES draw more attentions in recent years [1-4]. The energy input, transformation, output and the coupling relationship and uncertainty of each part in the DES need to be further studied in the modeling process.

Uncertainty could be roughly divided into two categories: random uncertainty and epistemic uncertainty. The former is impossible to erase but could be quantified by using the theory of probability. The random uncertainty is also called objective uncertainty. While the epistemic uncertainty stems from lack of knowledge, lack of data, cognitive deviation, etc., and which can be eliminated by sufficient data or in-depth study to improve, and is also called subjective uncertainty. In the DES design, the random uncertainty comes from the uncertainty of renewable energy output, and the epistemic uncertainty results from the analysis model. Since the random uncertainty of renewable energy output is inherent, designers try to reduce the epistemic uncertainty.

At present, the modeling methods of DES almost are theoretical model with simplification, which always deviate from reality. Compared to the traditional theoretical model, the data-driven model could reduce the complexity of the probability estimation and contribute to the accurate analytic solutions [5] .The data-driven model is mainly applied to system modeling[6], planning[7], short-term prediction[8, 9] and system control[10] currently. Meanwhile, with the development of the application of big data and the machine learning, the application of the data-driven model in the DES design is fit for solving the complex energy system.

Except for the improvement of the accuracy of the data-driven model, the reliability estimation in the DES design refers to the quantify uncertainty and the transmission of uncertainty. In this paper, the method to generate the reasonable distributions of the input meteorological parameters firstly. Then the accuracy of the theoretical model and the Back Propagation Neural network model (BP model) BP model was compared.

2. UNCERTAINTY ANALYSIS BASED ON PROBABILITY DENSITY ESTIMATION

Usually the input parameters are assumed to obey a certain distribution. In order to estimate reliability of complex energy system, the two main problems need to be solved, to quantify uncertainty and the transmission of uncertainty. The different types and sources of uncertainty could be quantitatively described by using the statistic method. The transmission of uncertainty is a major reason causing the uncertainty of energy system. The transmission of the uncertainty from inputs to the output response shows in Fig.1.

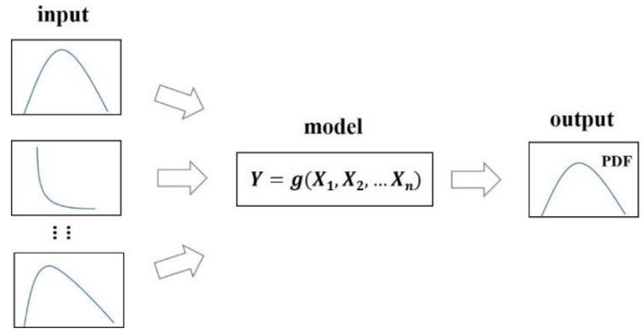

Fig.1 The transmission of the uncertainty

2.1 *Quantifying the input uncertainty*

The relationship of the input parameters contains the relevant variables and independent variables. Independent variables could be imported as stochastic distributions. While in the PV model, it is obvious that the input parameters are related. Table1 shows the Pearson Correlation Coefficients of the input parameters. The closer the correlation coefficient to 1 or -1, the stronger the correlation is, and the closer the correlation coefficient to 0, the weaker the correlation is. The relationships between global and diffuse radiation, temperature and relative humidity, temperature and global radiation are strong correlations. Thus, the reasonable distribution of the wind speed could be acquired by transforming hourly wind speed values to the probability density distribution. And the distributions of diffuse radiation and relative humidity could be acquired by calculating the marginal distribution of the global radiation and temperature respectively, the relationship of above-mentioned meteorological parameters are shown in Fig.2. While the detailed method to generate the uncertain global radiation and temperature were discussed in [11]. The flow of generating the distributions of meteorological parameters according to the historical data was shown in Fig.3.

Table1
Pearson Correlation Coefficients of the input parameters

	Wind speed	Global radiation	Diffuse radiation	Temperature	Relative humidity
Wind speed	1	0.072	0.064	0.046	-0.045
Global radiation	0.072	1	**0.564**	**0.514**	-0.391
Diffuse radiation	0.064	0.564	1	0.351	-0.298
Temperature	0.046	0.514	0.351	1	**-0.744**
Relative humidity	-0.045	-0391	-0.298	-0.744	1

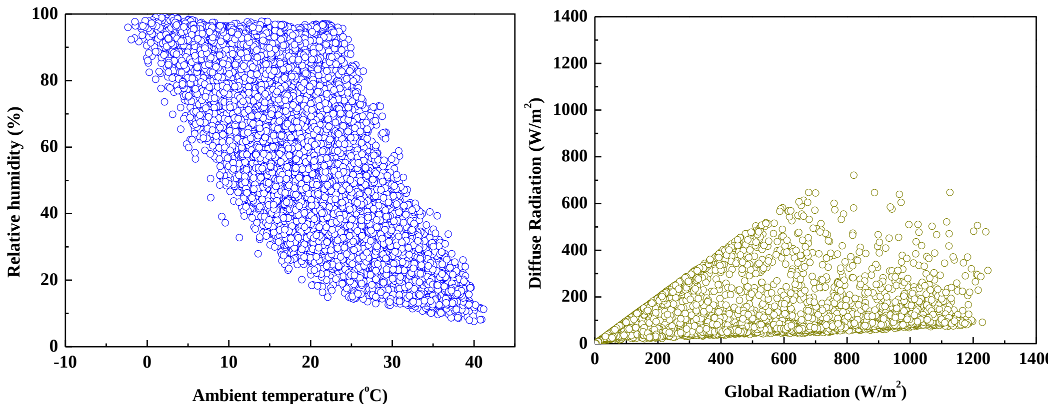

Fig.2 Meteorological parameter

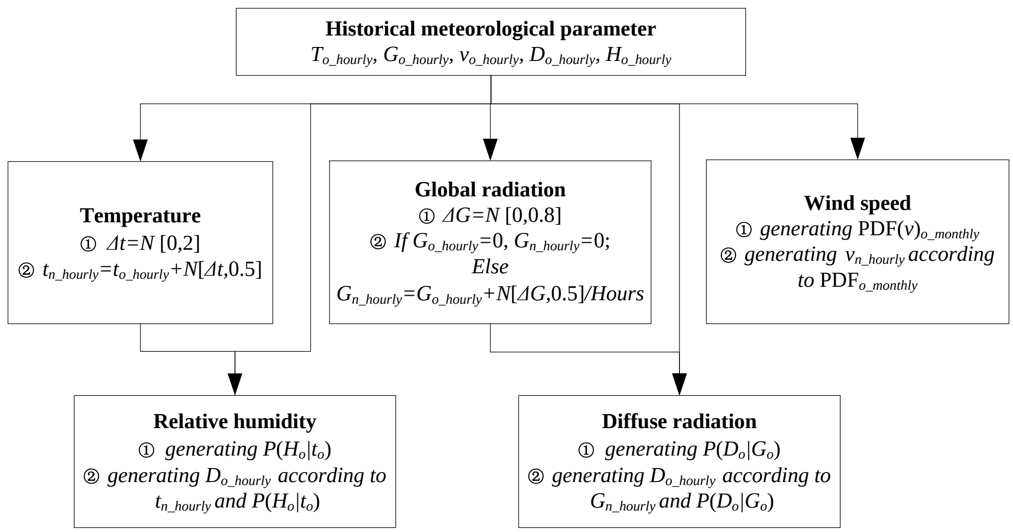

Fig.3 The flow of generating the distributions of meteorological parameters

2.2 Reliability estimation

In order to evaluate the reliability of the energy system, the first four order moments of the output response is obtained by numerical integration method, and by using Pearson method to estimate the probability density function of energy system output, and then calculate the reliability.

Monte Carlo Simulation (MCS) is the most commonly used numerical simulation method, by extracting multiple points to estimate probability density function, thus the failure probability of energy system could be estimated and the reliability estimation could be realized.

3. THEORETICAL MODEL AND BP MODEL

3.1 Theoretical model (TH model)

The thermal-electric coupled was developed according to the energy balance. The configuration of the PV module is based on a referenced monocrystalline PV module. The energy gain is the absorbed sunlight (P_{sun}), and the heat loss comprises radiative loss with the sky (P_{rad}), radiative loss with the ground or roof (P_{ground}), and convective loss with ambient ($P_{conv,top}$ +$P_{conv,bottom}$), the power output is recorded as P_{out}. For length reasons, the detailed theoretical model was presented in the previous published paper [5].

The energy balance equations of the referenced PV module are expressed in the following equations:

For the glass cover.

$$C_g\delta_g\rho_g\, \mathrm{d}T_g/\mathrm{d}\tau = P_{sun-g} - h_{v,g-a}(T_g - T_a) - h_{r,g-sky}(T_g - T_{sky}) - k_{g-EVA,1}(T_g - T_{EVA,1}) \tag{1}$$

here, the absorbed sunlight of glass cover could be written as,

$$P_{sun-g} = \int_0^{4.0} \mathrm{d}\lambda \varepsilon_g(\lambda,\theta) I_{AM\,1.5}(\lambda) \tag{2}$$

and the sky temperature is evaluated by the relation [12],

$$T_{sky} = 0.0552 T_a^{\,1.5} \tag{3}$$

For the first EVA layer.

$$C_{EVA,1}\delta_{EVA,1}\rho_{EVA,1}\,\mathrm{d}T_{EVA,1}/\mathrm{d}\tau = k_{g-EVA,1}(T_g - T_{EVA,1}) - k_{EVA,1-PV}(T_{EVA,1} - T_{PV}) \tag{4}$$

For the PV cell layer.

$$C_{PV}\delta_{PV}\rho_{PV}\,\mathrm{d}T_{PV}/\mathrm{d}\tau = P_{sun-PV} + k_{EVA,1-PV}(T_{EVA,1} - T_{PV}) - h_{PV-EVA,2}(T_{PV} - T_{EVA,2}) - P_{out} \tag{5}$$

here, the absorbed sunlight of glass cover could be written as,

$$P_{sun-PV} = \int_0^{4.0} \mathrm{d}\lambda\,\varepsilon_{PV}(\lambda,\theta)\tau_g(\lambda,\theta)I_{AM\,1.5}(\lambda) \tag{6}$$

where P_{out} is calculated according to the maximum power point tracking (MPPT) control with

$$P_{out} = (V \times I)_{mppt} \tag{7}$$

The current of a PV module can be expressed as function of voltage, by the expression derived from [13]:

$$I = I_{sc}[1 - c_1(\exp(V/c_2V_{oc}) - 1)] \tag{8}$$

where

$$c_1 = (1 - I_{mppt}/I_{sc})\exp(-V_{mppt}/c_2U_{oc}) \tag{9}$$

$$c_2 = (V_{mppt}/V_{oc} - 1)\left[1/\ln(1 - I_{mppt}/I_{sc})\right] \tag{10}$$

The coefficients c_1 and c_2 could be expressed as the relationship of the nameplate parameters of the PV module, which are listed in Table2. These parameters are obtained under standard test conditions (STC, G_{ref}=1000 W/m^2, T_{ref}=25 °C). Therefore, for realistic application, such parameters need to be modified according to the solar irradiance and panel temperature:

$$I_{sc} = (G/G_{ref})I_{sc,ref}[1 + k_I(T - T_{ref})] \tag{12}$$

$$V_{oc} = V_{oc,ref}[1 + k_V(T - T_{ref})] \tag{13}$$

$$I_m = (G/G_{ref})I_{m,ref}[1 + k_I(T - T_{ref})] \tag{14}$$

$$V_m = V_{m,ref}[1 + k_V(T - T_{ref})] \tag{15}$$

For the second EVA layer.

$$C_{EVA,2}\delta_{EVA,2}\rho_{EVA,2}\,\mathrm{d}T_{EVA,2}/\mathrm{d}\tau = k_{PV-EVA,2}(T_{PV} - T_{EVA,2}) - k_{EVA,2-ted}(T_{EVA,2} - T_{ted}) \tag{16}$$

For the tedlar layer.

$$C_{ted}\delta_{ted}\rho_{ted}\,\mathrm{d}T_{ted}/\mathrm{d}\tau = k_{EVA,2-ted}(T_{EVA,2} - T_{ted}) - h_{v,ted-a}(T_{ted} - T_a) - h_{r,ted-es}(T_{ted} - T_{es}) \tag{17}$$

Table 2
Nameplate parameters of the reference PV module

Panel rating (W)	Number of panels	V_{oc} (V)	I_{sc} (A)	V_{mppt} (V)	I_{mppt} (A)	Size (mm* mm)	k_V (%/ ℃)	k_I (%/ ℃)
165	30	52.7	9.79	43.4	9.21	2067*998	-0.29	+0.05

3.2 BP neural network model (BP model)

The numbers of nodes in the input, hidden and output layer of the BP model depend on the input and predicted values. In this paper, the main five meteorological parameters are provided as input parameters, and the only one as output parameter. The BP model topology in the power prediction model is shown in Fig.4.

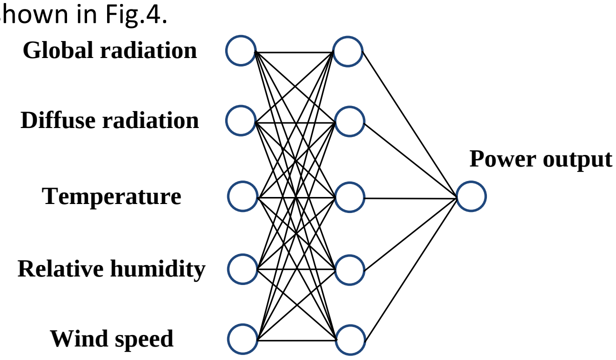

Fig.4 BP Neural network topology in the power prediction model

4. COMPARISON OF MODEL ACCURACY

The Desert Knowledge Australia Solar Centre (DKASC) is a real life demonstration of solar technologies spanning many types, ages, makes, models and configurations. And the monitoring data is available to researchers worldwide. The operating data of the polycrystalline Silicon with the installed capacity of 4.95kW (NO.11) were used as a reference.

The Mean Absolute Percentage Error (*MAPE*), Mean Square Percentage Error (*MSPE*) and Mean Standard Error (*MSE*) were selected to evaluate the accuracy of the forecasting models. The three evaluation index shows the degree that the forecasting results deviate from the actual values. The results show that the accuracy of the BP model is higher than that of the TH model. Moreover, the computational time consumed of the BP model is also much lower than the TH model, which takes 3,000 iterations to evaluate the panel temperature each time.

$$MAPE = \frac{1}{n}\sum_{i=1}^{n}\left|\frac{y_t^{'} - y_t}{y_t^{'}}\right| \times 100\% \tag{18}$$

$$MSPE = \frac{1}{n}\sqrt{\sum_{i=1}^{n}\left(\frac{y_t^{'} - y_t}{y_t^{'}}\right)^2} \times 100\% \tag{19}$$

$$MSE = \sqrt{\frac{\sum_{i=1}^{n}\left(y_t^{'} - y_t\right)^2}{n}} \tag{20}$$

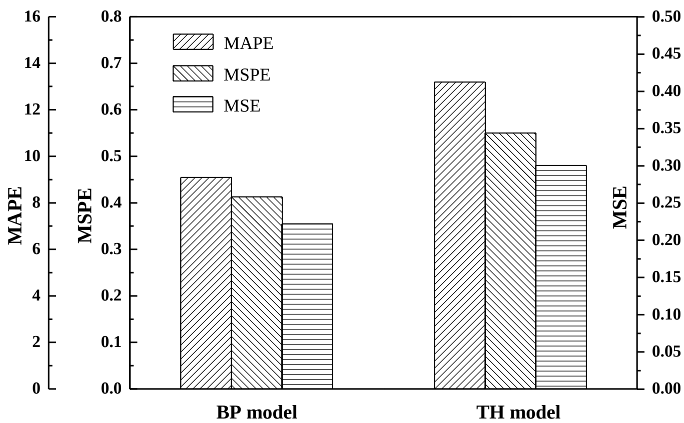

Fig.5 The accuracy comparison of the two models

5. COMPARISON OF THE TRANSMISSION OF THE UNCERTAINTY

Ideally, the best and worst cases need to be estimated in the design stage, while there is no persuasiveness to assess the uncertainty interval empirically. The Monte-Carlo Simulation involves the use of random numbers and probability to find solutions to complex problems. In this research, 100 groups of 8760 hourly random meteorological parameters were generated by using Monte-Carlo method. Then, the BP model and theoretical model were conducted to predict the generating capacity in a whole year. According to the results, taking the maximum and minimum power generation of each month to generate an interval, and comparing with real values over the years in Fig.6. The results show that the theoretical model overestimates the generating capacity while the BP model gives more appropriate estimation. In other words, the BP model was proved to be more accurate to estimate the uncertainty in the design stage.

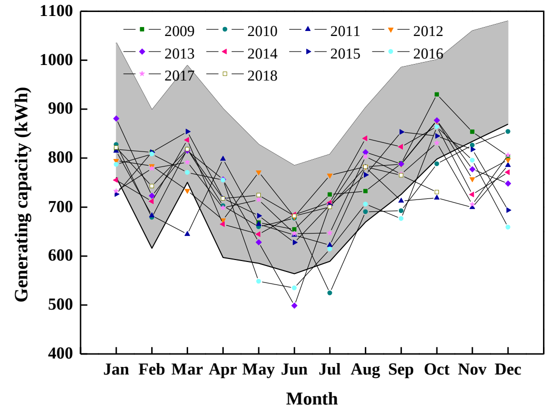

(a) TH model

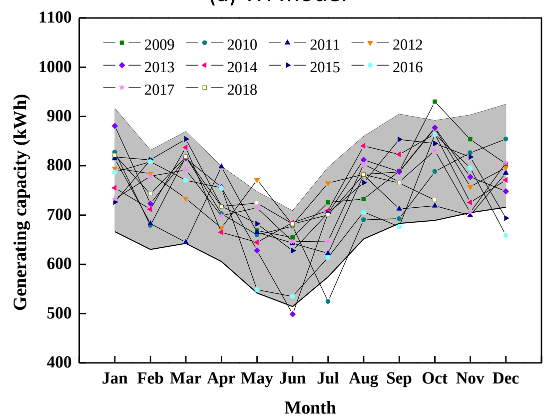

(b) BP model

Fig.6 Comparison of real generating capacity and predict values

Finally, the probability density functions argue that the uncertainty of output of BP model is obviously smaller than that of theoretical model, which is shown in Fig.7.

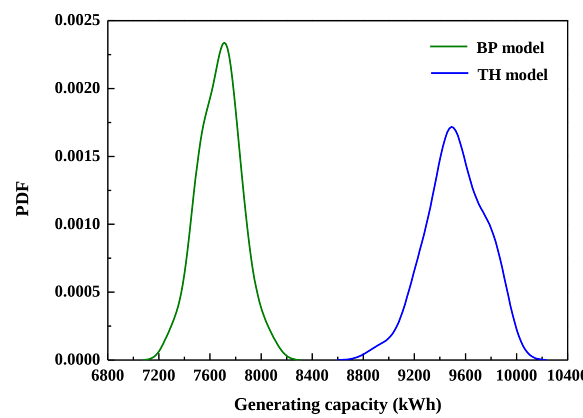

Fig.7 The probability density functions of BP model and TH model

6. CONCLUSIONS

The aim of this paper is to illustrate that the data-driven model is more suitable for estimating the system output than theoretical model under uncertainty. The BP model was selected as example. The method to improve the accuracy of the data-driven model is not including in this paper. Taking the photovoltaic system as example and the following conclusions are drawn:

(1)The comparison results argue that the uncertainty of output of BP model is obviously smaller than that of theoretical model.

(2)The BP model is more accurate to estimate the uncertainty in the design stage.

(3)The theoretical model overestimates the generating capacity in the PV system.

In this research, a simple study object was selected to demonstrate the simplicity and effectiveness of the data-driven model in the uncertainty estimation. With the increase of equipment type and quantity, the theoretical modeling gets more and more complicated. The data-driven model ignores the physical essence of the complicated system, and more accurate predictions can be made as long as there are enough historical data and reasonable distribution of input parameters. Finally, in the design stage, it also conclude that the predicted accuracy of the more advanced data-driven model could be further improved.

REFERENCE

[1] E. Mathioulakis, G. Panaras, V. Belessiotis. Uncertainty in estimating the performance of solar thermal systems. Solar Energy. 86 (2012) 3450-9.

[2] F. Domínguez-Muñoz, J.M. Cejudo-López, A. Carrillo-Andrés, C.R. Ruivo. Design of solar thermal systems under uncertainty. Energy and Buildings. 47 (2012) 474-84.

[3] G. Mavromatidis, K. Orehounig, J. Carmeliet. Uncertainty and global sensitivity analysis for the optimal design of distributed energy systems. Applied Energy. 214 (2018) 219-38.

[4] Z. Pang, Z. O'Neill. Uncertainty quantification and sensitivity analysis of the domestic hot water usage in hotels. Applied Energy. 232 (2018) 424-42.

[5] X. Fu, G. Li, X. Zhang, Z. Qiao. Failure probability estimation of the gas supply using a data-driven model in an integrated energy system. Applied Energy. 232 (2018) 704-14.

[6] C. Fan, F. Xiao, C. Yan, C. Liu, Z. Li, J. Wang. A novel methodology to explain and evaluate data-driven building energy performance models based on interpretable machine learning. Applied Energy. 235 (2019) 1551-60.

[7] C. Ye, Y. Ding, Y. Song, Z. Lin, L. Wang. A data driven multi-state model for distribution system flexible planning utilizing hierarchical parallel computing. Applied Energy. 232 (2018) 9-25.

[8] F. Ferracuti, A. Fonti, L. Ciabattoni, S. Pizzuti, A. Arteconi, L. Helsen, et al. Data-driven models for short-term thermal behaviour prediction in real buildings. Applied Energy. 204 (2017) 1375-87.

[9] N. Mohan, K.P. Soman, S. Sachin Kumar. A data-driven strategy for short-term electric load forecasting using dynamic mode decomposition model. Applied Energy. 232 (2018) 229-44.

[10] F. Smarra, A. Jain, T. de Rubeis, D. Ambrosini, A. D'Innocenzo, R. Mangharam. Data-driven model predictive control using random forests for building energy optimization and climate control. Applied Energy. 226 (2018) 1252-72.

[11] H. Li, J. Zhao, M. Li, S. Deng, Q. An, F. Wang. Performance analysis of passive cooling for photovoltaic modules and estimation of energy-saving potential. Solar Energy. 181 (2019) 70-82.

[12] W.C. Swinbank. Long - wave radiation from clear skies. Quarterly Journal of the Royal Meteorological Society. 89 (2010) 339-48.

[13] R.L. Chakrasali, V.R. Sheelavant, H.N. Nagaraja. Network approach to modeling and simulation of solar photovoltaic cell. Renewable & Sustainable Energy Reviews. 21 (2013) 84-8.

